Dynamics of the Auto-Ignition of Biogas in Turbulent Flows

Jhon Alexander Pareja Restrepo

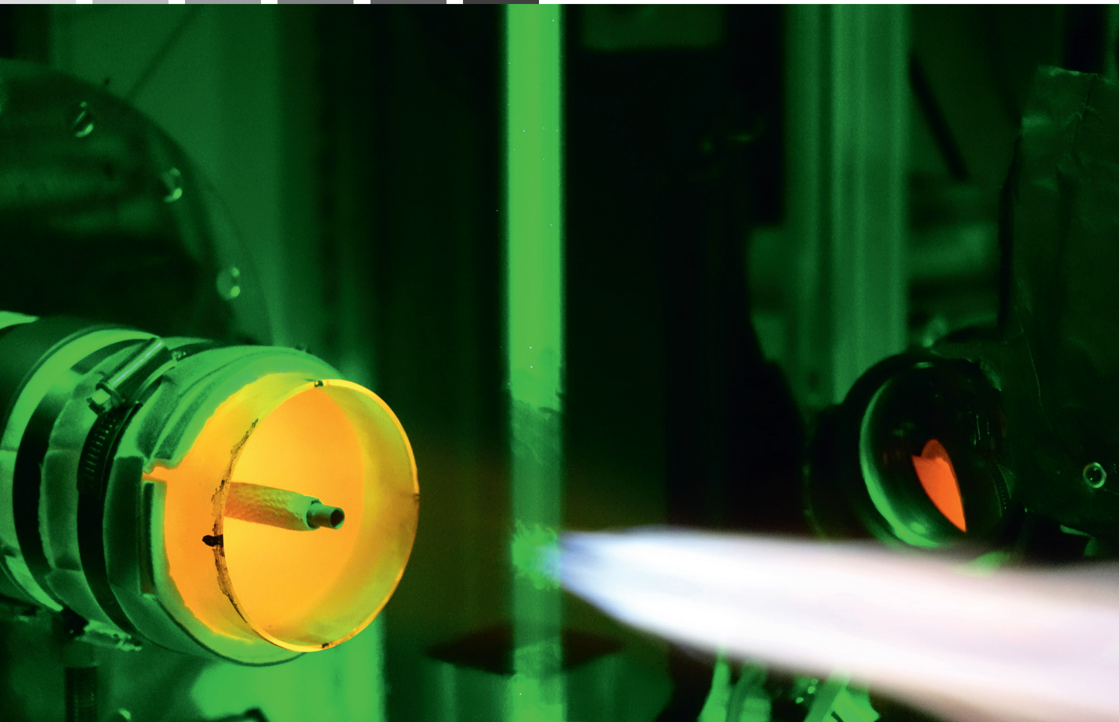

Dynamics of the Auto-Ignition of Biogas in Turbulent Flows

Dem Fachbereich Maschinenbau
an der Technischen Universität Darmstadt
zur
Erlangung des Grades eines Doktor-Ingenieurs (Dr.-Ing.)
eingereichte

D i s s e r t a t i o n

vorgelegt von

Jhon Alexander Pareja Restrepo, M.Sc.

aus Andes, Kolumbien

Berichterstatter:	Prof. Dr. habil. A. Dreizler
Mitberichterstatter:	Prof. Dr. habil. U. Maas
Tag der Einreichung:	15. April 2019
Tag der mündlichen Prüfung:	03. Juni 2019

Darmstadt 2019

D17

Messtechnik und Sensorik

Jhon Alexander Pareja Restrepo

Dynamics of the Auto-Ignition of Biogas in Turbulent Flows

D 17 (Diss. TU Darmstadt)

Shaker Verlag
Düren 2020

Bibliographic information published by the Deutsche Nationalbibliothek
The Deutsche Nationalbibliothek lists this publication in the Deutsche Nationalbibliografie; detailed bibliographic data are available in the Internet at http://dnb.d-nb.de.

Zugl.: Darmstadt, Techn. Univ., Diss., 2019

Printed in Germany.

ISBN 978-3-8440-7321-8
ISSN 1610-4773

Shaker Verlag GmbH • Am Langen Graben 15a • 52353 Düren
Phone: 0049/2421/99011-0 • Telefax: 0049/2421/99011-9
Internet: www.shaker.de • e-mail: info@shaker.de

Erklärung

Hiermit erkläre ich an Eides statt, dass ich die vorliegende Dissertation selbstständig verfasst und keine anderen als die von mir angegebenen Hilfsmittel verwendet habe. Ich erkläre außerdem, dass ich bisher noch keinen Promotionsversuch unternommen habe.

Jhon Alexander Pareja Restrepo　　　　Darmstadt, den 15. April 2019

Acknowledgements

This dissertation is a result of my work as research assistant at the *Institut Reaktive Strömungen und Messtechnik* (RSM), TU Darmstadt. First of all, I want to thank my advisor Prof. Andreas Dreizler, head of RSM, for giving the opportunity to carry out my research at his institute and for providing all necessary infrastructure and resources to perform the studies. I would like to thank him for his trust, support, recognition of my achievements, his encourage to continue working in the field and for his patience, particularly when the things did not go as expected.
I am very grateful to Prof. Ulrich Maas, director of the *Institut für Technische Thermodynamik* (ITT) – KIT, for kindly accepting to evaluate my thesis. It is a privilege to have someone of his knowledge and expertise on the combustion field interested in my work.
I am deeply grateful to my friend and colleague Ayane San, for all these years of joint work. I learned a lot from her, we enjoyed and suffered together in the lab during the long months of experimental setup and the long sleepless weeks of data recording. Her support was fundamental to complete this work. I would like to thank Felix Eitel, for transferring his knowledge on the test rig and to Benjamin Böhm for his kind support in obtaining all necessary resources and equipment. A special thanks goes to Tao Li, for the excellent joint work during the measurements campaigns that we carried out together and to Florian Zentgraf for the fruitful discussions and his support during the long hours of data recording of the last measurement campaign. I would like to acknowledge Wolfgang G. Bessler for providing a copy of the LIFSim program, Robert Schießl (ITT) for the fruitful discussions regarding NO-LIF, Frederik Fuest and Manuel Schütte (LaVision), for the collaboration that made the tomographic measurements possible. I would like to extend my gratitude to Andreas Ludwig for his support in the lab, to the people of the workshop, particularly to Roland and Dirk, for the parts and for providing ideas to improve the setups. I am grateful to all secretaries, but particularly to Marion for helping me with the administrative procedures. It is not possible to mention everyone in these few lines. However, I would like mention friends and colleagues, from the past and the present, for the nice working atmosphere: Norman, Matthias, Thabo, Benny, Michi, Tao, Flavia, Anna, Arne, Jan, Timo, Jean, Illya, Brian, Benny Bork, Jens, Ollie and Stritzke. The IT crew: Calli, Max, David and Andi, who solved my technical difficulties almost immediately. I would like to acknowledge Sandra Hartl (STFS) for performing the numerical simulations related to the work, Max, Cooper and Chris for proofreading some parts of the document and particularly Chris for adapting the figures of the fundamentals.
I am grateful to the Italian/Latin crew, the Colombians in Darmstadt and my long-time roommate Patrick for providing such a familiar atmosphere. My friends and relatives in Colombia and abroad, for the continuous support despite the distance. Last but not the least, I would like to thank my family: Olga, Guillermo, Julián, Andrés and Astrid, for their unconditional and loving support. They have always encourage me to pursuit my research interests, even though this has implied being so far away from home, for so many years. In particular, my deepest gratitude to my life partner Astrid, for her loving support, her invaluable efforts to overcome the thousands of kilometers between us, her understanding and encourage, especially during the writing of this thesis.

Darmstadt, April 2019 Jhon Alexander Pareja Restrepo

A mis padres, Olga y Guillermo

Abstract

For the development of future energy conversion concepts, sustainable, efficient combustion processes will continue to play a major role. A promising option is the use of renewable sources, such as biomass-derived gasses (biogas). In a variety of present combustion applications, auto-ignition is an essential process. This includes homogeneous charge compression ignition and diesel engines, and burners using flameless combustion. On the other hand, auto-ignition must be prevented in lean premixed pre-vaporized gas turbines or spark-ignition engines. In those practical devices, the fuel and oxidizer flows are highly turbulent. Therefore, understanding the complex, transient and three-dimensional turbulence-chemistry interactions underlying auto-ignition is of high relevance. For that purpose, this work presents an experimental study on auto-ignition of synthetic biogas (CH_4/CO_2 mixture). The experimental configuration consists of a fuel jet issuing into a high-turbulence, hot air co-flow to mimic conditions as those of practical devices. The study is focused on two main research aspects, instantaneous two-dimensional (2D) scalar field measurements during the onset of auto-ignition and time-resolved three-dimensional (3D) detection and tracking of auto-ignition kernels. For this purpose, advanced laser-optical diagnostics are adapted for simultaneous multi-parameter measurements.

Instantaneous 2D scalar fields of temperature, mixture fraction and scalar dissipation rate were derived by means of simultaneous Rayleigh scattering and planar laser-induced fluorescence of nitric oxide (NO-PLIF), which enables detecting auto-ignition events, and quantifying the corresponding local mixture fraction and temperature during the onset of auto-ignition. The analysis of these events experimentally confirmed previous fundamental findings from direct numerical simulations (DNS) and experiments which concluded that auto-ignition occurs preferentially in spots (kernels), on isocontours of the so-called most reactive mixture fraction, at locations with low scalar dissipation. A statistical evaluation of the effect of the boundary conditions on the auto-ignition characteristics of biogas showed that, for the presented configuration, neither the Reynolds number of the jet nor the co-flow temperature have a strong influence on the mixture fraction at which auto-ignition occurred. Additionally, it was found that the high level of local anisotropy prevented the onset of auto-ignition.

Regarding 3D transient phenomena, time-resolved tomographic LIF of the hydroxyl radical OH, which combines volumetric laser illumination with a multi-camera detection, was used to study the 3D size, structure, location, and orientation of synthetic biogas auto-ignition kernels and their temporal evolution. Results showed that auto-ignitions occurred in well-defined radial regions of the 3D flow, with strong fluctuations in the main direction of the flow. The statistical evaluation of the orientation and growth of auto-ignition kernels with respect to the mean flow field revealed that the kernels were oriented tangentially to the main flow direction and temporally evolved towards this preferential direction as the ignition event progressed.

Findings derived from the results of the presented work will contribute to better understand the fundamentals of auto-ignition processes and will provide experimental data for validation of numerical simulations and the development and improvement of models.

Kurzzusammenfassung

In der Entwicklung zukünftiger Energiewandlungskonzepte werden nachhaltige, effiziente Verbrennungsprozesse weiterhin eine wesentliche Rolle spielen. Eine vielversprechende Option liegt in der Verwendung erneuerbarer Energieträger, wie beispielsweise in aus Biomasse hergestelltem Gas (Biogas). In einer Vielzahl heutiger Verbrennungsanwendungen ist Selbstzündung ein unverzichtbarer Prozess. Das schließt homogene Kompressionszündung und Dieselmotoren ein, sowie Brenner die flammenlose Verbrennung nutzen. Demgegenüber muss Selbstzündung in mager vorgemischten Gasturbinen oder Ottomotoren vermieden werden. In diesen praxisrelevanten Systemen sind die Strömungen von Brennstoff und Oxidator hochgradig turbulent. Daher ist ein Verständnis der komplexen, transienten und dreidimensionalen Turbulenz-Chemie-Interaktionen, die der Selbstzündung zugrunde liegen, von wesentlicher Bedeutung. Zu diesem Zweck wird in dieser Arbeit eine experimentelle Untersuchung der Selbstzündung von synthetischem Biogas (CH4/CO2 Mischung) vorgestellt. Der Versuchsaufbau besteht aus einem Brennstoffjet, der in einen hochturbulenten, heißen Coflow aus Luft eingeströmt wird, um die Betriebsbedingungen praxisnaher Apparate nachzubilden. Die Untersuchung legt Gewicht auf zwei wesentliche Aspekte, die zweidimensionale (2D) Messung der Momentanwerte von Skalarfeldern während der Entstehung von Selbstzündung und die zeitaufgelöste, dreidimensionale (3D) Detektion und Verfolgung von Selbstzündungskernen. Dazu werden fortschrittliche Lasermesstechniken für eine simultane Multiparametererfassung adaptiert.

Momentanwerte der 2D-Skalarfelder von Temperatur, Mischungsbruch und skalarer Dissipationsrate wurden mittels simultaner Rayleigh-Streuung und ebener Laser-induzierter Fluoreszenz an Stickstoffmonoxid (NO-PLIF) abgeleitet. Dies ermöglicht die Detektion von Selbstzündungsereignissen sowie eine Quantifizierung der entsprechenden lokalen Mischungsbrüche und Temperaturen während der Entstehung von Selbstzündung. Eine Auswertung dieser Ereignisse bestätigte experimentell frühere, grundlegende Erkenntnisse aus direkter numerischer Simulation sowie aus Experimenten, die schlussfolgerten, dass Selbstzündung vorzugsweise in Punkten (sog. Kernen) auftritt, an Isolinien des sogenannten reaktivsten Mischungsbruches, an Stellen mit niedriger skalarer Dissipation. Eine statistische Bewertung des Einflusses der Randbedingungen auf die Selbstzündungscharakteristik von Biogas zeigte, dass, für die vorgestellte Konfiguration, weder die Reynoldszahl des Brennstoffjets, noch die Temperatur der Gleichströmung einen großen Einfluss auf den Mischungsbruch haben, an dem Selbstzündung auftritt. Zusätzlich wurde festgestellt, dass ein hoher Grad an lokaler Anisotropie das Eintreten von Selbstzündung verhindert.

Im Hinblick auf transiente 3D-Phänomene wurde eine zeitaufgelöste, tomographische LIF am Hydroxylradikal OH angewendet, die volumetrische Laserbeleuchtung mit einer Mehr-Kamera-Detektion verbindet, um die 3D-Größe, Struktur, Lage und Orientierung von Selbstzündungskernen in synthetischem Biogas zu untersuchen sowie deren zeitliche Entwicklung. Die Ergebnisse zeigen, dass Selbstzündungen in wohldefinierten radialen Regionen der 3D-Strömung auftreten, mit starken Fluktuationen in die Hauptströmungsrichtung. Die statistische Bewertung der Orientierung und des Wachstums der Selbstzündungskerne bezogen auf das mittlere Strömungsfeld zeigte auf, dass die Kerne tangential

zur Hauptströmungsrichtung ausgerichtet sind und sich zeitlich zu dieser Vorzugsrichtung entwickeln während das Selbstzündungsereignis fortschreitet.

Die Erkenntnisse, die aus den Ergebnissen der vorgestellten Arbeit abgeleitet sind, werden dazu beitragen die Grundlagen von Selbstzündungsprozessen besser zu verstehen und werden Experimentaldaten zur Validierung numerischer Simulationen bereitstellen sowie für das Entwickeln und Verbessern von Modellen.

Contents

Nomenclature

Acronyms

	Description
AI	Auto-Ignition
CCD	Charge-Couple Device
CL	Chemiluminescence
F10	Fuel Blend 90 vol.-% CH_4/10 vol.-% CO_2
F20	Fuel Blend 80 vol.-% CH_4/20 vol.-% CO_2
F30	Fuel Blend 70 vol.-% CH_4/30 vol.-% CO_2
F40	Fuel Blend 60 vol.-% CH_4/40 vol.-% CO_2
F50	Fuel Blend 50 vol.-% CH_4/50 vol.-% CO_2
FCU	Flow Conditioning Unit
FOV	Field of View
FWHM	Full Width at Half Maximum
IRO	Intensified Relay Optics
JCF	Jet-in-Cross-Flow
JHC	Jet-in-Hot-Coflow
LIF	Laser-Induced fluorescence
LOH	Lift-off-Height
LSF	Line-Spread Function
HT	High Temperature
LT	Low Temperature
MT	Medium Temperature
MTF	Modulation Transfer Function
MWPH	Microwave Plasma Heater
NOx	Nitric Oxides
PIV	Particle Image Velocimetry
PLIF	Planar Laser-Induced Fluorescence

	Description
PSF	Point-Spread Function
SMART	Simultaneous Multiplicative Algebraic Reconstruction Technique
SNR	Signal-to-Noise Ratio
SRF	Step Response Function
SVD	Singular Value Decomposition

Greek Symbols

	Description	Unit
δ	Outer length scale	mm
$\delta_{0.05}$	Local outer scale full-width where u reaches 5% of u_c	mm
$\delta_{1/2}$	Local half-width at half-maximum of velocity profile	mm
∇I_T	3D gradient of tomographic OH signal intensity	a.u.
$\mathit{\Gamma}$	Normalized spectral overlap fraction	-
κ_ν	Spectral absorption coefficient	cm^{-1}
Λ	Scaling constant for turbulent round jets	-
λ_D	Strain-limited scalar diffusion scale	μm
λ_B	Batchelor scale	μm
λ_{MW}	Microwave wavelength of the test rig	m
ξ	Mixture fraction	-
ξ_{AI}	Auto-ignition mixture fraction	-
ξ_{cl}	Centerline mixture fraction	-
ξ_{MR}	Most reactive mixture fraction	-
ξ_{NO}	Mixture fraction from NO-PLIF	-
ξ_{Ray}	Mixture fraction from Rayleigh scattering	-
ξ_{st}	Stoichiometric mixture fraction	-
ρ_{coflow}	Co-flow density	Kgm^{-3}
ρ_{jet}	Jet density	Kgm^{-3}
σ_{di}	Standard deviation of d_i	mm
σ_{air}	Differential Rayleigh scattering cross-section of air	-
σ_{CH4}	Differential Rayleigh scattering cross-section of methane	-
σ_{CO2}	Differential Rayleigh scattering cross-section of carbon dioxide	-
σ_{fuel}	Differential Rayleigh scattering cross-section of the fuel	-
σ_{He}	Differential Rayleigh scattering cross-section of helium	-

	Description	Unit
σ_i	Differential Rayleigh scattering cross-section of the species i	-
σ_{mix}	Mixture-averaged differential Rayleigh scattering cross-section	-
σ_{N2}	Differential Rayleigh scattering cross-section of nitrogen	-
σ_{ox}	Differential Rayleigh scattering cross-section of the oxidizer	-
θ	Momentum radius	mm
ν_{coflow}	Kinematic viscosity of the co-flow	m^2s^{-1}
ν_{jet}	Kinematic viscosity of the fuel jet	m^2s^{-1}
χ	Scalar dissipation rate	s^{-1}
χ_{AI}	Scalar dissipation rate at auto-ignition zone	s^{-1}
χ_x	Scalar dissipation rate axial component	s^{-1}
χ_y	Scalar dissipation rate radial component	s^{-1}

Latin Symbols

	Description	Unit
A_j	Einstein coefficient for spontaneous emission	s^{-1}
A_{opt}	Rayleigh scattering collection system efficiency	-
B_{12}	Einstein coefficient for stimulated absorption	$m^3J^{-1}s^{-2}$
$\overline{BG_{HT}}$	Background signal at high temperature	a.u.
$\overline{BG_{Ray}}$	Rayleigh background signal	a.u.
$\overline{BG_{RT}}$	Background signal at room temperature	a.u.
C_{opt}	NO-PLIF collection system efficiency	-
D_{coflow}	Coflow nozzle outer diameter	mm
$D_{coflow,hyd}$	Coflow nozzle hydraulic diameter	mm
d_i	Displacement of a kernel pair along the i-direction	mm
$D_{i,coflow}$	Coflow nozzle inner diameter	mm
$\overline{d}_i$	Mean of d_i	mm
$D_{j,c}$	Mass diffusivity of jet in the co-flow	m^2s^{-1}
d_{jet}	Jet nozzle diameter	mm
$d_r = (d_y^2 + d_z^2)^2$	Displacement of a kernel pair along the radial direction	mm
E	Shot-to-shot laser energy reference	a.u.
$\boldsymbol{e_r}$	Unit vector along radial direction	-
$\boldsymbol{e_x}$	Unit vector along axial direction	-

	Description	Unit
f_B	Boltzmann fraction of molecules in the grounds state	-
I_{bg}	CL background signal intensity of the "no-flame" region	a.u.
I_{flame}	Characteristic CL signal intensity of the flame region	a.u.
I_ν^0	Normalized spectral laser irradiance	$\mathrm{Wcm^{-2}cm^{-1}}$
I_{surf}	OH signal level for AI kernels detection	a.u.
I_{thresh}	Adaptive CL signal intensity threshold	a.u.
I_T	Tomographic reconstructed OH signal intensity	a.u.
J_0	Source momentum flux	N
k	Boltzmann constant	$\mathrm{JK^{-1}}$
$\mathrm{K}_{i,j}$	i-th kernel detected in the j-th shot	-
k_r	Angle between $\boldsymbol{l_1}$and $\boldsymbol{e_r}$	rad
k_x	Angle between $\boldsymbol{l_1}$ and $\boldsymbol{e_x}$	rad
$\boldsymbol{l_1}$	Vector along the major axis of a kernel fixed coordinate	-
l_i	Feret diameter along the i-direction	mm
$\dot{m}$	Mass flow rate	$\mathrm{Kgs^{-1}}$
$\dot{m}_{axial}$	Axial air injection mass flow rate	$\mathrm{Kgs^{-1}}$
$\dot{m}_{coflow}$	Co-flow mass flow rate	$\mathrm{Kgs^{-1}}$
$\dot{m}_{cool}$	Cooling air mass flow rate	$\mathrm{Kgs^{-1}}$
$\dot{m}_{jet}$	Jet mass flow rate	$\mathrm{Kgs^{-1}}$
$\dot{m}_{seeding}$	Seeding air mass flow rate	$\mathrm{Kgs^{-1}}$
$\dot{m}_{tang}$	Tangential air mass flow rate	$\mathrm{Kgs^{-1}}$
N	Number density	$\mathrm{m^{-3}}$
N_K	Number of kernels used for any computation	-
N_{NO}	Number density of NO	$\mathrm{m^{-3}}$
P	Pressure	Pa
P_{80}	80th percentile	-
P_{LOH}	Accumulative probability of the LOH	-
p_{thresh}	CL threshold level	%
Q	Electronic quenching rate	$\mathrm{s^{-1}}$
Re_{coflow}	Bulk Reynolds number of the co-flow	-
Re_δ	Outer Reynolds number	-
Re_{jet}	Bulk Reynolds number of the jet	-
$\overline{S_{G,air}}$	Mean air reference raw signal	a.u.
S_N	NO fluorescence signal intensity	a.u.
$S_{N,ox}$	NO fluorescence signal intensity of the oxidizer	a.u.
S_R	Rayleigh scattering signal intensity	a.u.
$\overline{S_{R,air}}$	Air reference Rayleigh measurement	a.u.

	Description	Unit
S_{Ratio}	Normalized Rayleigh signal	a.u.
$\overline{S_{R,He}}$	Helium reference Rayleigh measurement	a.u.
T	Temperature	K
T_{AI}	Auto-ignition temperature	K
T_{coflow}	Co-flow temperature	K
$T_{control}$	Co-flow control temperature	K
T_{jet}	Fuel jet temperature	K
U	Absolute streamwise velocity	ms^{-1}
u	Excess streamwise velocity	ms^{-1}
U_{coflow}	Bulk exit velocity of the co-flow	ms^{-1}
u_c	Local outer excess centerline velocity	ms^{-1}
U_{jet}	Bulk exit velocity of the jet	ms^{-1}
W_{fuel}	Molecular weight of the fuel	gmol^{-1}
W_{mix}	Molecular weight of the mixture	gmol^{-1}
W_{NO}	Molecular weight of NO	gmol^{-1}
W_{ox}	Molecular weight of the oxidizer	gmol^{-1}
x	Axial x-coordinate	mm
X_{fuel}	Mole fraction of the fuel	-
X_i	Mole fraction of the species i	-
y	y-coordinate	mm
Y_{fuel}	Mass fraction of the fuel	-
$Y_{fuel,0}$	Mass fraction of the fuel at the nozzel exit	-
Y_{NO}	Mass fraction of NO	-
$Y_{NO,fuel}$	Mass fraction of NO in the fuel	-
$Y_{NO,ox}$	Mass fraction of NO in the oxidizer	-
z	z-coordinate	mm

Dimensionless Numbers

	Description
Re	Reynolds number
Sc	Schmidt number